sustainability

MDPI

Article

Land Cover Based Landscape Pattern Dynamics of Anhui Province Using GlobCover and MCD12Q1 Global Land Cover Products

Jinling Zhao [1], Jie Wang [2], Yu Jin [2], Lingling Fan [2], Chao Xu [1], Dong Liang [1] and Linsheng Huang [1,*]

[1] National Joint Engineering Research Center for Analysis and Application of Agro-Ecological Big Data, Anhui University, Hefei 230601, China; aling0123@163.com (J.Z.); graymagpie@163.com (C.X.); dliang@ahu.edu.cn (D.L.)

[2] Key Laboratory of Intelligent Computing & Signal Processing, Ministry of Education, Anhui University, Hefei 230039, China; jwangahu@163.com (J.W.); ahuJingy@163.com (Y.J.); Fanlingahu@163.com (L.F.)

* Correspondence: linsheng0808@163.com

Received: 4 April 2018; Accepted: 20 April 2018; Published: 22 April 2018

Abstract: The development and free distribution of global land cover (GLC) products have greatly assisted in the evolution and analysis of relationships between land cover and landscape pattern. In this study, GlobCover and MCD12Q1 GLC datasets of 2005 and 2009 were comparatively used to analyze the variation of land cover in Anhui Province, China at both the class and landscape scale. The land cover classification schemes of both datasets were firstly reclassified to six types of forestland, grassland, wetland, cropland, artificial area, and others, and then FRAGSTATS was used to calculate the landscape indices. The results showed that from 2005 to 2009, the area density of 'cropland' landscape decreased, and it increased for 'wetland' and 'artificial area'. The landscape fragmentation of 'forestland' and 'grassland' were larger. Moreover, over the same period, the class edge (CE) of 'cropland' was diminished; while the CE of 'wetland' was enhanced and the aggregation became larger. Conversely, the aggregation and shape complexity of 'artificial area' remained the same. The clumpiness index (CLUMPY) of 'cropland' varied from 0.8995 to 0.9050, indicating a higher aggregation and more concentrated distribution. The heterogeneity index (HT) value of MCD12Q1 and GlobCover datasets varied, respectively, from 0.9642 to 0.9053 and from 0.8867 to 0.8751, demonstrating that the landscape heterogeneity of Anhui Province was reduced from 2005 to 2009. Driving force analysis (DFA) was just performed for 'artificial area', 'cropland', and 'wetland' according to the 2005–2009 statistical yearbook data, because they were apt to be affected by human activities over a relatively short period of time.

Keywords: landscape pattern; global land cover; GlobCover; MCD12Q1

1. Introduction

Landscape ecology is largely founded on the notion that environmental patterns strongly influence ecological processes [1]. It is a rapidly growing science of quantifying the ways in which ecosystems interact, of establishing a link between activities in one region and repercussions in another region [2]. As a part and a focus of landscape ecology, landscape pattern has been paid more attention. Landscape pattern mainly refers to the shape, ratio, and spatial features of landscape elements, and the basic characteristics is landscape heterogeneity [3]. It can be quantified in a variety of ways depending on the type of data collected, the manner in which it is collected, and the objectives of the investigation [4–6]. At a large spatial scale, the development and integration of remote sensing (RS), geographic information system (GIS), and global positioning system (GPS) have greatly facilitated the evolution and quantification of landscape pattern analysis [7–9]. Land cover is generally considered to be the important ecological indicator for investigating the Earth′s resources and many studies have been performed concerning such an issue [10]. Consequently, analysis of spatial variations in landscape patterns of land cover can be very useful for evaluating the regional ecological system qualitatively and quantitatively.

In recent years, many studies have focused on analyzing the characteristics and dynamic changes of landscape patterns in urban-suburban areas, agriculture, forest, dryland, wetland, etc., through various remote sensing imagery. Vogelmann et al. [11] investigated the effects of Landsat 5 Thematic Mapper (TM) and Landsat 7 Enhanced Thematic Mapper Plus (ETM+) radiometric and geometric calibrations and corrections on landscape characterization. Fichera et al. [12] characterized the dynamics of land cover pattern and its changes during a fifty-year period (1954–2004), using the aerial photos (1954), and Landsat scenes (Multispectral Scanner (MSS) 1975, TM 1985 and 1993, ETM+ 2004). Li et al. [13] investigated how landscape composition and configuration would affect urban heat island (UHI) in the Shanghai metropolitan region of China, based on the analysis of land surface temperature (LST) in relation to normalized difference vegetation index (NDVI), vegetation fraction (Fv), and percent impervious surface area (ISA). Qian et al. [14] quantified spatiotemporal pattern of urban greenspace using the most commonly used Landsat TM data with 30 m resolution and 2.5 m high spatial resolution imagery. del Castillo et al. [15] analyzed the spatiotemporal changes in forest cover in Moncayo Natural Park (Spain) from 1987 to 2010 using RS techniques, GIS and quantitative indices of landscape ecology. It is obvious that most studies have been performed on the evaluation of landscape pattern and changes therein with respect to a certain land cover type. Conversely, it is just highly crucial to evaluate the landscape pattern of primary land cover types at provincial, national, continental, and even global scales. The development of remote sensing has facilitated the identification of land cover and the assessment of landscape pattern [16–19].

Identification of land cover types is always the first requisite to monitor and evaluate the landscape pattern [20]. The continuous development of global land cover (GLC) products, depending on remote sensing technology, has provided the land cover classification datasets at regional and global scales. Some typical GLC products have been widely used to investigate landscape pattern, such as the International Geosphere–Biosphere Program Data and Information Systems (IGBP-DIS) [21], University of Maryland (UMD) [22], Moderate Resolution Imaging Spectroradiometer (MODIS) Collection 5.1 Land Cover type (hereafter referred to as MCD12Q1) [23], GLC2000 [24], GlobCover [25], and GlobeLand30 [26]. GLC products are usually produced using different remotely sensed imagery (sensors), methodologies, and validation techniques. It has become increasingly significant to evaluate the landscape pattern dynamics of land cover by harmonizing multi-source and multitemporal GLC products.

To measure or quantify the landscape pattern, it is necessary to select and calculate appropriate indicators or 'metrics' through readily available data and software [27,28]. According to the characteristics of remotely sensed imagery, some studies have been carried out to characterize the landscape pattern and its dynamics of land use and land cover (LULC) using multi-stage remote sensing images and built-up patch density metrics. Ji et al. [29] characterized long-term trends and patterns of urban sprawl using both the remotely sensed data and landscape metrics. Gillanders et al. [30] identified potential and the limitations of landscape pattern indices for land cover spatial pattern analysis using three or more image dates. Zhang et al. [31] investigated the relation between soil erosion and landscape patterns using 12 landscape indices (patch index, patch cohesion index, modified Simpson's evenness index, and the aggregation index) in FRAGSTATS. In summarizing, the scale effect that the landscape response of LULC can be better revealed within appropriate spatial units. Selection of landscape pattern indices greatly depends on the spatial distribution of study objectives and landscape effect. In addition, FRAGSTATS has been widely used in exploring the landscape pattern of remote sensed based LULC, due to its popularity and good compatibility with ArcGIS.

In our study, Anhui Province, China is used as the study area and two typical GLC products of MCD12Q1 2005/2009 and GlobCover 2005/2009 are selected. When harmonizing the land cover types due to different land cover classification schemes (LCCSs), the changes in landscape patterns of primary land cover types are investigated qualitatively and quantitatively at both the class and landscape scale using the landscape structure analysis software FRAGSTATS 4.2. Additionally, the driving force analysis (DFA) of some susceptible land cover types is also performed to assist in finding out the primary influence factors.

2. Materials and Methods

2.1. Study Area

Anhui Province is located in the mid-latitude zone of east China at 114°54′~119°37′ E longitude and 29°41′ ~34°38′ N latitude (Figure 1a). It is about 450 km wide from east to west, with a north-south length of 570 km, and a total area of 139 thousand and 600 km^2, which lies in the hinterland of the Yangtze River Delta. The province is situated in the transition zone from alternating subtropical to temperate zone, with a mild and humid climate characterized by four distinct seasons. There are three main geomorphic features: plains (Huaihe & Yanjiang); hills (Jianghuai, southern Anhui & western hills); and mountains (Western mountainous region). It is a relatively ideal pilot area to assess the availability and possibility of investigating the land cover based landscape patterns using the GLC products. As a big agricultural province, cropland is the top land use type in the study area. The province is geographically divided by the Yangtze and Huaihe rivers into three natural areas of Wanzhong, Wanbei, and Wannan (Figure 1b).

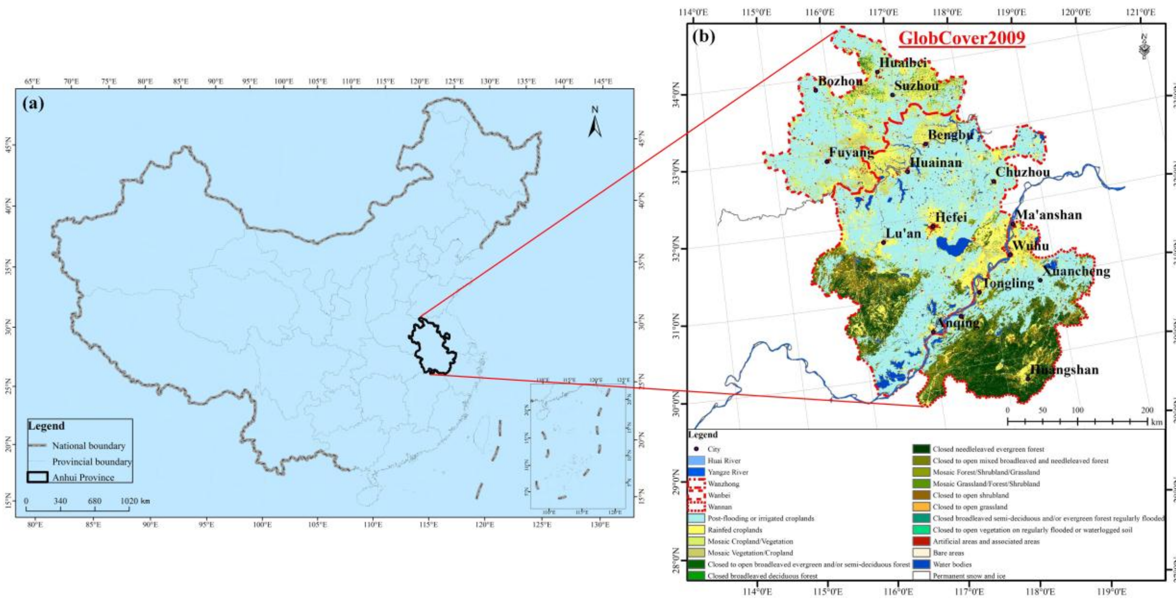

Figure 1. Geographic location (**a**) and land cover types and subdivisions (**b**) of Anhui Province, China.

2.2. Technical Route

Several steps are required to finish the dynamic monitoring of land cover based landscape patterns on a provincial scale (Figure 2). The MODIS Reprojection Tool (MRT) is firstly used to finish the preprocessing of MCD12Q1 including imaging mosaicking, projection transformation, data format conversion. Two datasets of MCD12Q1 2005/2009 and GlobCover 2005/2009 are jointly processed to form a unified basis by image subsetting, projection transformation, and resampling. Subsequently, landscape indices at both the class and landscape scale are selected to dynamically analyze the land cover based landscape patterns, according to the landscape features of the study area. Finally, DFA is performed to explain the landscape pattern dynamics of 'artificial area', 'cropland', and 'wetland'.

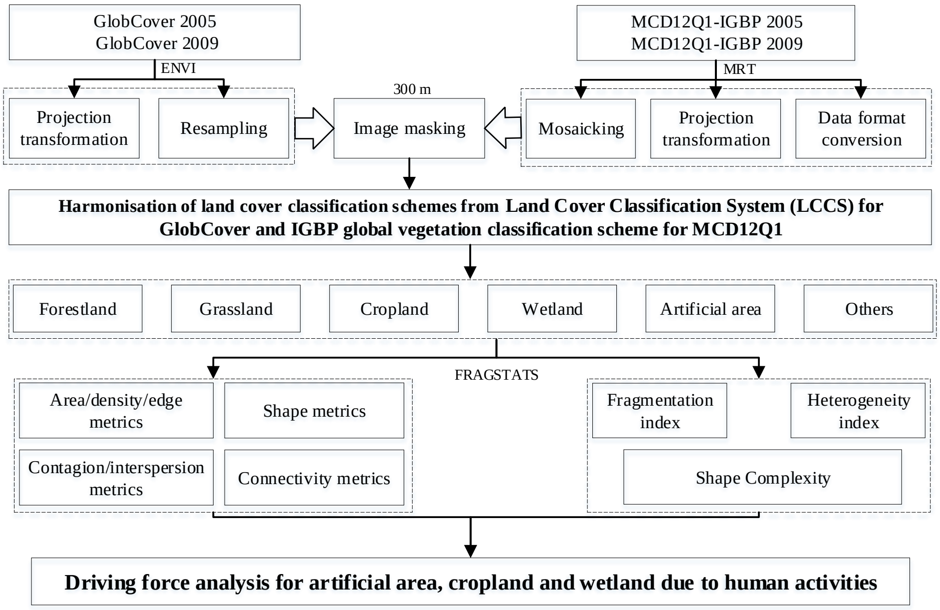

Figure 2. General workflow chart in this study.

2.3. Data Sources and Preprocessing

Considering the spatial-temporal availability of current GLC maps, two kinds of GLC products were selected including GlobCover and MCD12Q1 (Table 1). GlobCover products have just two periods of 2005 and 2009, while MCD 12Q1 has successive temporal coverage (V051) during 2001–2013. Consequently, we have to select the years of 2005 and 2009. In addition, both of the datasets have relatively nearest spatial resolution in comparison with other GLC products.

Table 1. Summarization and comparison of MCD12Q1 and GlobCover.

	MCD12Q1	**GlobCover**
Sensor	MODIS Terra+Aqua	ENVISAT MERIS
Collection date	January 2001/2013–December 2001/2013	December 2004–June 2006
Spatial resolution	500 m	300 m
Input data	Terra- and Aqua-MODIS data	13 Spectral bands and NDVI composites
Method	Supervised decision-tree classification method	Per-pixel supervised (urban and wetland) and unsupervised classification
Validation method	Statistical validation	Statistical validation
Total accuracy	74.8%	73%

2.3.1. MCD12Q1 Products and Pre-Treatment

MCD12Q1 provides data characterizing five global land cover classification systems. They describe land cover properties derived from observations spanning a year's input of observation data from the Terra and Aqua satellites applied to depict land cover types. Specifically, the five land cover classification systems are respectively IGBP global vegetation classification scheme (Land Cover Type 1), UMD scheme (Land Cover Type 2), MODIS-derived leaf area index (LAI) and fraction of photosynthetically active radiation (LAI/fPAR) scheme (Land Cover Type 3), MODIS-derived net primary production (NPP) scheme (Land Cover Type 4), and plant functional type (PFT) scheme (Land Cover Type 5). Land Cover Type 1 is considered the optimum scheme to study the land cover in Anhui Province, China [32].

To cover the whole study area, four scenes are required with the track numbers of h27v05, h27v06, h28v05, and h28v06. The original MCD12Q1 products are stored in hierarchical data format (HDF) with the sinusoidal (SIN) projection. It is highly necessary to perform some preprocessing for matching the GlobCover products. MRT was employed to finish the image mosaicking, format conversion, reprojection, and resampling. Here, the MODIS HDF was converted into Geotiff, while the projection was converted from SIN to World Geodetic System 1984 (WGS84)/Universal Transverse Mercator (UTM). In addition, the image subsetting and reclassification were also completed in ENVI (ENvironment for Visualizing Images).

2.3.2. GlobCover Products and Pre-Treatment

GlobCover 2005 (covering December 2004–June 2006), the first 300 m GLC product, was released by the European Space Agency (ESA) in 2008. GlobCover 2009 (covering January–December 2009) was released on 21 December 2010. These data are derived from the 300 m medium resolution imaging spectrometer (MERIS) sensor, on board the ENVISAT satellite mission based on a multi-dimensional iterative clustering algorithm. MERIS was built by the ESA at the Cannes Mandelieu Space Center located in both the towns of Cannes and Mandelieu in France. The GLC product includes 22 land cover types, according to the LCCS and the overall classification accuracy is 73%. The available GlobCover product has been produced using the WGS84 datum and is freely distributed in the Geotiff format. It was firstly projected to the UTM coordinate system, and then was just preprocessed by subsetting the image and reassigning digital number (DN) values to the reclassified land cover types. To match the minimum spatial resolution of 500 m of MCD12Q1, it was resampled to 500 m from the original resolution of 300 m using the nearest-neighbor resampling method.

2.3.3. Harmonization of LCCSs

To generate comparable GLC maps, it is highly necessary to reclassify the land cover categories due to different classification schemes. A total of six land cover types were acquired in ENVI by harmonizing the various LCCSs for both GlobCover and MCD12Q1 (Table 2). The original land cover types were reclassified into 'forestland, 'grassland', 'cropland', 'wetland', 'artificial area', and 'others'. In our study, the decision tree was constructed to achieve our goal in ENVI [33].

Table 2. Harmonized LCCS derived from both GlobCover and MCD12Q1.

Land Cover Type	GlobCover	MCD12Q1
Forestland	1. Closed to open broadleaved evergreen and/or semi-deciduous forest 2. Closed broadleaved deciduous forest 3. Closed needleleaved evergreen forest 4. Closed to open mixed broadleaved and needleleaved forest 5. Mosaic forest/shrubland/grassland 6. Closed broadleaved semi-deciduous and/or evergreen forest regularly flooded 7. Closed to open shrubland	1. Evergreen needleleaf forest 2. Evergreen broadleaf forest 3. Deciduous needleleaf forest 4. Deciduous broadleaf forest 5. Mixed forests 6. Closed shrublands 7. Open shrublands
Grassland	1. Mosaic grassland/forest/shrubland 2. Closed to open grassland	1. Woody savannas 2. Savannas 3. Grasslands
Cropland	1. Post-flooding or irrigated croplands 2. Rainfed croplands 3. Mosaic cropland/vegetation 4. Mosaic vegetation/cropland	1. Croplands 2. Cropland—natural vegetation mosaic

Table 2. *Cont.*

Wetland	1. Closed to open vegetation on regularly flooded or waterlogged soil 2. Water bodies 3. Permanent snow and ice	1. Water bodies 2. Permanent wetlands 3. Snow and ice
Artificial area	1. Artificial areas and associated areas	1. Urban areas
Others	1. Bare areas	1. Barren or sparsely vegetated

2.4. Selection of Landscape Metrics at Both the Class and Landscape Scale

To effectively realize the evolution analysis of regional landscape pattern, it is necessary to select the appropriate landscape indices [34–37]. The dynamics of landscape pattern on land cover in Anhui Province was characterized, using the landscape structure analysis software FRAGSTATS 4.2, defining patches using a four-neighbor rule. FRAGSTATS is a computer software program designed to compute a wide variety of landscape metrics for categorical map patterns [38]. Metrics are grouped to six types according to the aspect of landscape pattern measured. They are area and edge metrics, shape metrics, core area metrics, contrast metrics, aggregation metrics, and diversity metrics. Within each of these groups, metrics are further grouped into patch, class, and landscape metrics. In this way, we selected the landscape indices at both the class and landscape scale by comprehensively considering the structure and composition of landscape and regional scale effect (Table 3).

Table 3. Description of the selected landscape metrics used in the study.

Landscape Metrics	Metric	Acronym
Area/density/edge metrics	Class area	CA
Area/density/edge metrics	Number of patches	NP
Area/density/edge metrics	Patch density	PD
Area/density/edge metrics	Edge density	ED
Area/density/edge metrics	Landscape shape index	LSI
Shape metrics	Perimeter-area fractal dimension index	PAFRAC
Contagion/interspersion metrics	Clumpiness index	CLUMPY
Contagion/interspersion metrics	Interspersion and juxtaposition index	IJI
Connectivity metrics	Patch cohesion index	COHESION
Fragmentation	Fragmentation index	F
Heterogeneity	Heterogeneity index	HT
Shape Complexity	Mean patch fractal dimension	MPFD

1. *CA, NP, and PD*

CA (Equation (1)) is fundamental measures of landscape composition; specifically, how much of the landscape is comprised of a particular patch type [39]. *NP* (Equation (2)) simply measures the extent of subdivision or fragmentation of the patch type. *PD* (Equation (3)) is a limited, but fundamental, aspect of landscape pattern. The corresponding formulae are given below

$$CA = \sum_{j=1}^{n} a_{ij}\left(\frac{1}{10,000}\right) \tag{1}$$

$$NP = n_i \tag{2}$$

$$PD = \frac{n_i}{A}(10,000)(100) \tag{3}$$

where a_{ij} is the area of patch ij; A is the total landscape area; and n_i is the number of patches in the landscape of patch type (class) i.

2. *ED, LSI, and PAFRAC*

ED (Equation (4)) measures the edge length over the unit area. *LSI* (Equation (5)) measures the perimeter-to-area ratio for the landscape as a whole, which is identical to the habitat diversity index [40]. *PAFRAC* (Equation (6)) is appealing because it reflects shape complexity across a range of spatial scales (patch sizes) [41]. The relevant equations are

$$ED = \frac{\sum_{k=1}^{m} e_{ik}{}^{*}}{A}(10,000) \tag{4}$$

$$LSI = \frac{0.25\sum_{k=1}^{m} e_{ik}{}^{*}}{\sqrt{A}} \tag{5}$$

$$PAFRAC = \frac{\frac{2}{[n_i \sum_{j=1}^{n} (\ln p_{ij} \cdot \ln a_{ij})] - [(\sum_{j=1}^{n} \ln p_{ij})(\sum_{j=1}^{n} \ln a_{ij})]}}{(n_i \sum_{j=1}^{n} \ln p_{ij}^2) - (\sum_{j=1}^{n} \ln p_{ij})^2} \tag{6}$$

where e_{ik} is the total length of edge in landscape between patch types (classes) i and k; e_i is the total length of the patch edge of the i type; a_{ij} is the ij type patch area; and p_{ij} is the perimeter (m) *of* patch ij.

3. Aggregation Index

CLUMPY (Equations (7) and (8)) is a class-level only metric computed such that it ranges from -1 when the patch type is maximally disaggregated to 1 when the patch type is maximally clumped [42]. It is calculated from the adjacency matrix, which shows the frequency with which different pairs of patch types appear side-by-side on the map. *IJI* (Equation (9)) is based on patch adjacencies, not cell adjacencies like the contagion index [43]. The corresponding equations are

$$Given\ G_i = \left[\frac{g_{ii}}{(\sum_{k=1}^{m} g_{ik})}\right] \tag{7}$$

$$CLUMPY = \left[\begin{array}{c} \frac{G_i - P_i}{1-P_i} \quad for\ G_i \geq P_i \\ g \\ \frac{G_i - P_i}{1-P_i} \quad for\ G_i < P_i;\ P_i \geq 0.5 \\ \frac{P_i - G_i}{-P_i} \quad for\ G_i < P_i;\ P_i < 0.5 \end{array}\right] \tag{8}$$

$$IJI = \frac{-\sum_{k=1}^{m}\left[\left[\frac{e_{ik}}{\sum_{k=1}^{m} e_{ik}}\right] \ln \left[\frac{e_{ik}}{\sum_{k=1}^{m} e_{ik}}\right]\right]}{\ln(m-1)}(100) \tag{9}$$

where g_{ii} is the number of like adjacencies (joins) between pixels of patch type (class) i based on the double-count method.; g_{ik} is the number of adjacencies (joins) between pixels of patch type (class) i and k based on the double-count method; P_i is the proportion of the landscape occupied by patch type (class) i; e_{ik} is the sum of the edge lengths between the i and k type patches, and m is the number of patch types (classes) present in the landscape.

4. Connectivity Index

COHESION (Equation (10)) measures the physical connectedness of the corresponding patch type as [44]

$$COHESION = \left[1 - \frac{\sum_{j=1}^{n} p_{ij}^{*}}{\sum_{j=1}^{n} p_{ij}^{*}\sqrt{a_{ij}^{*}}} \cdot \left[1 - \frac{1}{\sqrt{Z}}\right]^{-1}\right] \cdot (100) \tag{10}$$

where p_{ij}^{*} is the perimeter of patch ij in terms of number of cell surfaces; a_{ij}^{*} is the area of patch ij in terms of number of cells; and Z is the total number of cells in the landscape.

5. Metric Selection of Spatial Landscape Pattern

In this section, F (Equation (11)), HT (Equation (12)), and $MPFD$ (Equation (13)) were selected to study the spatial pattern of landscape pattern in Anhui Province. Here, F is a quantitative index to determine the degree of landscape fragmentation, which characterizes the degree of disturbance of human activities and is related to biodiversity. HT characterizes the complexity of the landscape, by analyzing its composition and function. $MPFD$ is another measure of shape complexity. Mean fractal dimension approaches one for shapes with simple perimeters and approaches two when shapes are more complex [45]. The corresponding formulae are

$$F = \frac{P}{Q} \tag{11}$$

$$HT = -\sum_{i=1}^{m} p_i \log_2 p_i \tag{12}$$

$$MPFD = \frac{\left\{\sum_{i=1}^{m}\sum_{j=1}^{n} 2\ln\left(\frac{0.25p_{ij}}{\ln a_{ij}}\right)\right\}}{N} \tag{13}$$

where P is the number of patches of the landscape; Q is the area average of the landscape type; P_i is the i type of patch area to whole landscape area proportion; m is the type of landscape; P_{ij} is the patch perimeter of type ij, in units of m; a_{ij} is the patch area of type ij; and N is the number of patches of a certain type.

3. Results and Discussion

3.1. Reclassified Land Cover Maps Derived from MCD 12Q1 and GlobCover

As shown in Figure 3, from 2005 to 2009, there are some differences for the reclassification results between MCD12Q1 and GlobCover. For example, it is obvious that the 'forestland' area of MCD12Q1 is larger than that of GlobCover, while they have similar values for 'grassland', 'cropland', 'wetland' and 'artificial area'. Take the map of 2005 as the example, the areas of 'forestland', 'grassland', 'cropland', 'wetland', and 'artificial area' are 32,202.25 km^2, 7643.75 km^2, 93,398.25 km^2, 4943.50 km^2, 2090.25 km^2, respectively, while they are 26,370.50 km^2, 6788.75 km^2, 100,106.80 km^2, 5510.75 km^2, 1835.00 km^2, respectively. The differences are −5831.75 km^2, −855.00 km^2, 6708.55 km^2, 567.25 km^2, −255.25 km^2. We can find that there are significant differences for 'forestland' and 'cropland' in comparison with other types.

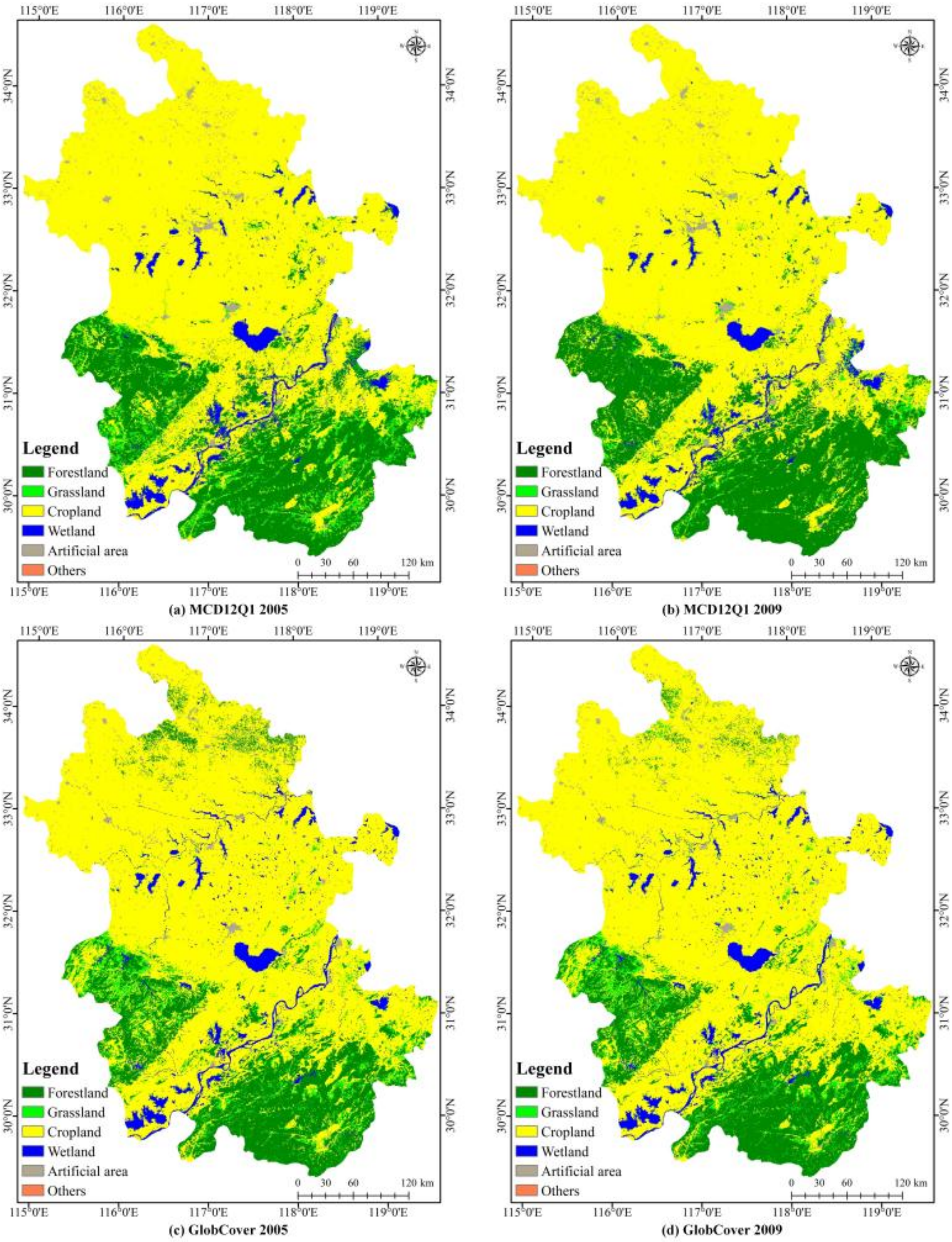

Figure 3. Land cover reclassification of MCD12Q1 and GlobCover in 2005 and 2009.

3.2. Analysis of Landscape Pattern Change

3.2.1. Comparison of *CA*, *NP*, and *PD*

In ArcGIS, the image format of the four land cover images from 2005 to 2009 was converted into a grid of 500 × 500 m grid cells. In addition, the *CA*, *NP* and *PD* were calculated by FRAGSTATS 4.2 on the scale pattern of landscape patches, as shown in Table 4. For the 'forestland', the *CA*, *NP*, and *PD* of MCD12Q1 are significantly increasing, while the *CA* of GlobCover is decreasing and the *NP* and *PD* are increasing. The two datasets also show different trends for the 'grassland'. The *CA* of MCD12Q1 is greatly increasing, whereas the *NP* and *PD* are markedly reducing. Conversely, the *CA*, *NP*, and *PD* of GlobCover have a slightly increasing trend. For the 'cropland', the trend of the two datasets is the same, with the values increasing and the *NP* and *PD* slightly reducing. For the 'wetland', the *CA* of both datasets demonstrate a decreasing tendency, in contrast to the increasing *NP* and *PD*.

These changes are particularly apparent in the GlobCover. For the ‘artificial area’, the two indices of the two datasets are minimal. For the ‘others’, the increasing value of MCD12Q1 is trending opposite to the *NP* and *PD*. The three indices of GlobCover are increasing, and the *CA*, *NP*, and *PD* of MCD12Q1 for both periods are comparatively larger. In summarizing, the increase and decrease of *CA* for ‘cropland’ and ‘wetland’, respectively, are opposite to the *NP* and *PD*.

Table 4. Analysis of the patch number and patch density based on MCD12Q1 and GlobCover in Anhui Province (2005–2009).

Land Cover Type	Dataset	*CA* (km^2)		*NP* (Account)		*PD* (Per km^2)	
		2005	2009	2005	2009	2005	2009
Forestland	MCD12Q1	32,202.25	34,658.00	3753	3099	1.45	2.41
	GlobCover	26,370.50	25,068.75	3257	3443	1.21	1.28
Grassland	MCD12Q1	7643.75	3995.50	7359	6262	2.83	1.19
	GlobCover	6788.75	6985.75	6135	7025	2.29	2.62
Cropland	MCD12Q1	93,398.25	94,844.25	2482	2457	0.96	0.95
	GlobCover	100,106.75	101,400.50	2252	2061	0.84	0.77
Wetland	MCD12Q1	4943.50	4630.50	1684	1809	0.65	0.70
	GlobCover	5510.75	5318.75	1527	1589	0.57	0.59
Artificial area	MCD12Q1	2090.25	2090.25	1221	1221	0.47	0.47
	GlobCover	1835.00	1795.75	861	866	0.32	0.32
Others	MCD12Q1	388.00	447.50	834	718	0.32	0.28
	GlobCover	14.75	57.00	30	122	0.01	0.05

In 2005, the order of the values based on MCD12Q1 was ‘cropland’ > ‘forestland’ > ‘grassland’ > ‘wetland’ > ‘artificial area’ > ‘others’, and in 2009, the order was ‘cropland’ > forestland’ > ‘wetland’ > ‘artificial area’ > ‘others’, indicating ‘cropland’ and ‘grassland’ patch type area is expanding, whereas, ‘forestland’ patch type area is greatly reduced. In 2005, the order of *NP* and *PD* values based on MCD12Q1 was ‘grassland’ > ‘forestland’ > ‘cropland’ > ‘wetland’ > ‘artificial area’ > ‘others’, and in 2009, the order was ‘forestland’ > ‘grassland’ > ‘cropland’ > ‘wetland’ > ‘artificial area’ > ‘others’, indicating the number of patches is increasing in ‘forestland’, while, in contrast, ‘grassland’ patch number reduced. However, based on the GlobCover, the *CA*, *NP*, and *PD* of the sequence are unchanged, and the specific gravity is low, and the two data results are different.

In order to further measure the degree of landscape fragmentation, the landscape fragmentation index F_{i} is introduced. The formula is

$$F_i = \frac{P_i}{Q} \tag{14}$$

where P_{i} is the number of patches of the *i*th type, and Q is the average of the area of all landscape types.

As shown in Table 5, a comprehensive analysis by combining the landscape index and landscape fragmentation, can be found that the F_{i} value changes in the ‘forestland’, ‘grassland’, and ‘others’ during the four years is larger, the F_{i} change of ‘cropland’ and ‘wetland’ is very small, and the F_{i} value of ‘artificial area’ almost remained unchanged. The results show that the corresponding index change trend of the landscape type, with a smaller change of the value of F_{i} is more consistent with the change of the *NP* and *PD* of the two datasets. The change of the F_{i} is larger, the inconsistency of the corresponding index change trend is bigger. Although the spatial resolution of the MCD12Q1 and GlobCover data are resampled to 500 m, the scale effect, due to the significantly different LCCSs, can still affect the analysis of landscape fragmentation when the landscape pattern evolution analysis is carried out in an area with a large landscape fragmentation. Therefore, the two datasets show a significant difference in the analysis results.

Table 5. Analysis of landscape fragmentation metrics between MCD12Q1 and GlobCover in Anhui Province (2005–2009).

Land Use Type	Dataset	F_i	
		2005	**2009**
Forestland	MCD12Q1	0.1601	0.2671
	GlobCover	0.1390	0.1469
Grassland	MCD12Q1	0.3139	0.1322
	GlobCover	0.2618	0.2997
Cropland	MCD12Q1	0.1059	0.1048
	GlobCover	0.0961	0.0879
Wetland	MCD12Q1	0.0718	0.0772
	GlobCover	0.0652	0.0678
Artificial area	MCD12Q1	0.0521	0.0521
	GlobCover	0.0367	0.0369
Others	MCD12Q1	0.0356	0.0306
	GlobCover	0.0013	0.0052

3.2.2. Comparison of *ED*, *LSI*, and *PAFRAC*

As shown in Table 6, through the horizontal comparison of *ED* and *LSI* of Anhui Province in 2005–2009, we obtain a similar trend with the *NP* and *PD*. For the 'forestland', the *ED* of MCD12Q1 is decreasing, while the *LSI* and *PAFRAC* are increasing, indicating that the landscape edge of 'forestland' is decreasing, and the dispersion and shape complexity increasing. The *ED*, *LSI*, and *PAFRAC* of GlobCover are reduced, indicating that the edge of the landscape, dispersion and shape complexity are all reduced. For the 'grassland', the same three values of MCD12Q1 are reduced, while the *ED* and *LSI* of GlobCover are increased, and the *PAFRAC* decreases, indicating that the shape complexity of 'grassland' is diminished. For the 'cropland', the trend of the two datasets are the same, and the three values are smaller. For the 'wetland', the three values of the two datasets become larger. For the 'artificial area', the two values of the two datasets are minimal. For the 'others' type, the *ED* and *PAFRAC* of MCD12Q1 become larger, and the *LSI* becomes smaller. The three values of GlobCover become larger, and the *LSI* and *PAFRAC* of MCD12Q1 for both periods (2005 and 2009) are larger than those of the corresponding GlobCover.

Table 6. Analysis of edge density and shape metrics between MCD12Q1 and GlobCover in Anhui Province (2005–2009).

Land Cover Type	Dataset	*ED* (m/km^2)		*LSI*		*PAFRAC*	
		2005	**2009**	**2005**	**2009**	**2005**	**2009**
Forestland	MCD12Q1	174.84	89.72	64.5933	92.5138	1.5381	1.6042
	GlobCover	168.26	154.00	70.7938	66.4795	1.5321	1.5228
Grassland	MCD12Q1	149.30	139.21	111.3514	49.9141	1.6202	1.5429
	GlobCover	123.65	130.26	101.0030	104.8776	1.5904	1.5848
Cropland	MCD12Q1	181.98	164.39	40.2682	36.3044	1.5147	1.5116
	GlobCover	215.86	193.10	47.3705	42.2951	1.5393	1.5280
Wetland	MCD12Q1	43.61	46.79	40.6348	44.9817	1.5004	1.5116
	GlobCover	42.55	42.14	38.9788	39.2500	1.4453	1.4555
Artificial area	MCD12Q1	27.32	27.34	38.8852	38.9235	1.4221	1.4226
	GlobCover	18.74	18.42	29.5000	29.3471	1.2614	1.2481
Others	MCD12Q1	9.81	10.34	32.4304	31.7176	1.5864	1.6081
	GlobCover	0.33	1.36	5.5625	11.7419	1.2862	1.5031

At the same time, the *ED*, *LSI*, and *PAFRAC* of the different land cover types of the same data in Table 6 were compared vertically. As shown in Figure 4, we can get the order change of the three indices from large to small in four years. The proportion of the three exponential values for each land cover type based on GlobCover varies little, while the *ED* and *LSI* based on MCD12Q1 vary widely.

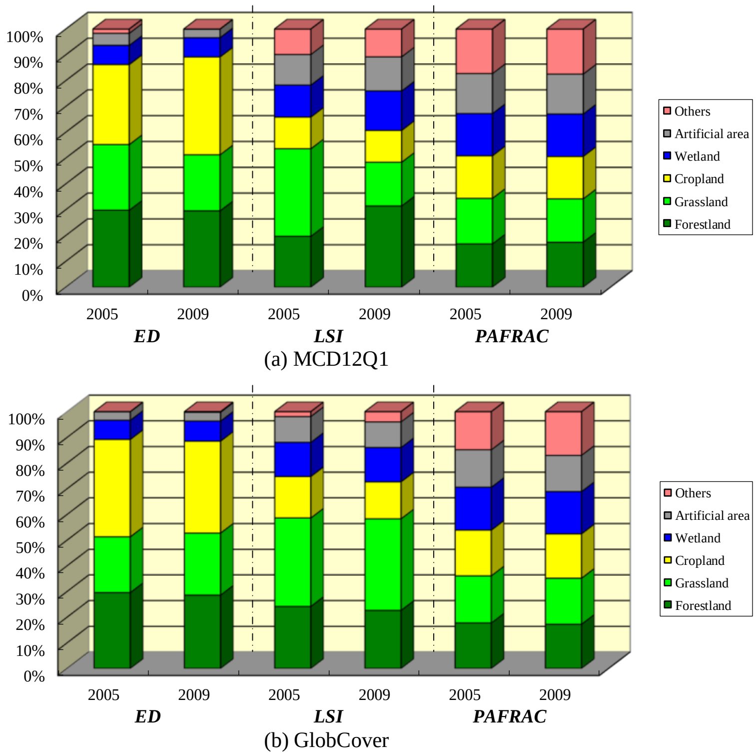

Figure 4. Comparison of the edge density and shape metrics based on (**a**) MCD12Q1 and (**b**) GlobCover, in Anhui Province (2005–2009).

The order based on the size of the two datasets are 'cropland' > 'forestland' > 'grassland' > 'wetland' > 'artificial area' > 'others'. However, within the four years, according to MCD12Q1, 'cropland' significantly increased and 'grassland' significantly reduced, whereas comparatively smaller changes in these land cover types were apparent, when viewing the GlobCover. This indicates that the edge length of 'cropland' in MCD12Q1 is larger in the unit area, and that of 'grassland' between the heterogeneous landscape elements in the unit area is smaller. At the same time, compared with GlobCover, 'grassland' in MCD12Q1 was significantly smaller over the four years, and 'cropland' became larger, indicating that the shape of 'grassland' tends to be regular and the distribution is more concentrated, the shape becomes irregular, and the distribution becomes more dispersed. While the two datasets were not significantly changed, that is, the complexity of patch shape did not change significantly.

3.2.3. Comparison of Aggregation

As shown in Table 7, the *CLUMPY* of 'forestland' in MCD12Q1 are reduced from 0.7971, in 2005, to 0.2585 in 2009. Also, patch types tend to be randomly distributed, while the degree of aggregation decreases and the *IJI* increases from 0.6032, in 2005, to 0.6471 in 2009, indicating that the number of adjacent patch types has increased. The *CLUMPY* and *IJI* of 'forestland' in GlobCover increase over the four-year period, indicating that in 2009, both the degree of aggregation of the patch types and the number of adjacent patch types increased compared to 2005. MCD12Q1 and GlobCover show a different trend for *CLUMPY*, which is due to measuring the clustering index using the node matrix. The scale and resolution of the image granularity will affect the number of nodes and, hence, the *CLUMPY* may vary, according to the scale used. Likewise, the *CLUMPY* of the two datasets also show different trends in the region of the larger area of landscape fragmentation, such as 'grassland' and 'others', where the *IJI* becomes larger and adjacent. The number of patch types increased, while 'cropland', 'wetland', and 'artificial area', with a smaller landscape fragmentation, showed the same cluster index. By comparing the *CLUMPY* and *IJI* of the two datasets in Table 7, the differences in the *CLUMPY* of the 'forestland' and 'grassland' between the two datasets are evident, and for 'cropland', the *IJI* of the difference has also very significant changes (Figure 5).

Table 7. Comparison of contagion and interspersion metrics based on MCD12Q1 and GlobCover data in Anhui Province (2005–2009).

Land Cover Type	Dataset	*CLUMPY*		*IJI* (%)	
		2005	**2009**	**2005**	**2009**
Forestland	MCD12Q1	0.7971	0.2585	60.32	64.71
	GlobCover	0.7608	0.7709	48.24	48.80
Grassland	MCD12Q1	0.3455	0.8479	56.08	62.67
	GlobCover	0.3728	0.3568	49.76	54.91
Cropland	MCD12Q1	0.8995	0.9095	79.55	78.76
	GlobCover	0.8829	0.8956	75.39	78.39
Wetland	MCD12Q1	0.7098	0.6675	79.70	79.14
	GlobCover	0.7370	0.7303	36.77	45.12
Artificial area	MCD12Q1	0.5774	0.5770	19.93	21.39
	GlobCover	0.6598	0.6582	27.87	28.38
Others	MCD12Q1	0.1779	0.2516	75.20	78.15
	GlobCover	0.2843	0.2163	41.33	48.51

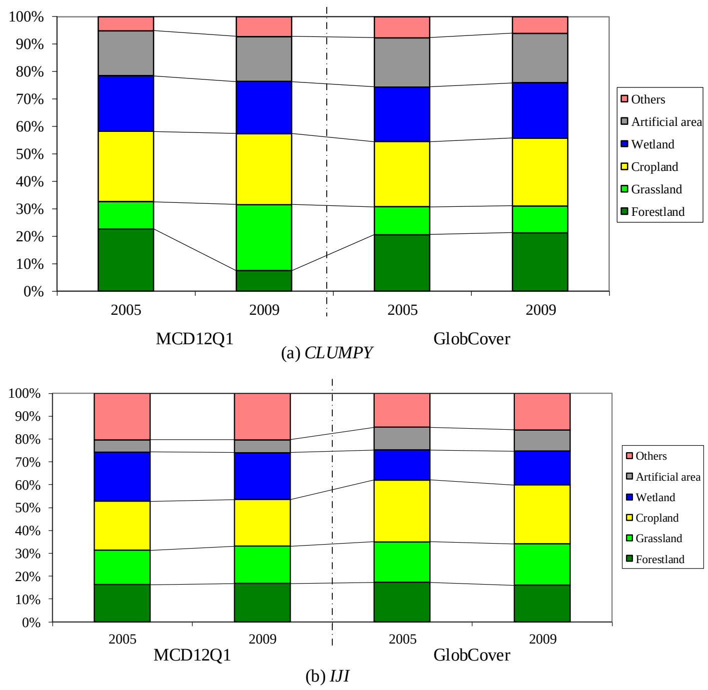

Figure 5. Analysis of contagion and interspersion metrics of Anhui Province (2005–2009).

3.2.4. Connectivity Comparison

This section chooses *COHESION* to study the connectivity of landscape patches. As shown in Table 8, the *COHESION* of the 'forestland' in MCD12Q1 dropped from 99.35 in 2005 to 62.12 in 2009, indicating the distribution became more and more broken. Conversely, the 'forestland' of *COHESION* in GlobCover slightly increased from 99.14 to 99.22. The results of two datasets are different, due to the spatial resolution and the LCCSs. The same reason also results in different results for the 'grassland' and 'others' of the two datasets. The *COHESION* of 'cropland', 'wetland', and 'artificial area' show negligible change, and have a higher patch cohesion index, and the natural connectivity is better and the distribution is greater.

Table 8. Analysis of landscape connection based on MCD12Q1 and GlobCover in Anhui Province.

Land Cover Type	Dataset	*COHESION*	
		2005	**2009**
Forestland	MCD12Q1	99.35	62.12
	GlobCover	99.14	99.22
Grassland	MCD12Q1	80.08	99.49
	GlobCover	78.81	77.71
Cropland	MCD12Q1	99.81	99.80
	GlobCover	99.84	99.85
Wetland	MCD12Q1	92.17	89.52
	GlobCover	93.12	92.92
Artificial area	MCD12Q1	78.64	78.65
	GlobCover	75.78	75.15
Others	MCD12Q1	37.45	55.42
	GlobCover	31.83	37.17

3.2.5. Analysis of Spatial Landscape Pattern

In this section, the landscape pattern of Anhui Province is analyzed by using MCD12Q1 and GlobCover, and the landscape index of the above landscape-scale is analyzed. Table 9 lists the changes of *F*, *HT*, and *MPFD* over the period 2005–2009. The *F* value of MCD12Q1 was reduced from 0.0668 in 2005 to 0.0600 in 2009, while that of GlobCover increased from 0.0524 in 2005 to 0.0563 in 2009. It is shown that the fragmentation of landscape in Anhui Province is smaller, the GlobCover data becomes larger in MCD12Q1, and the fragmentation index of MCD12Q1 is larger than that of GlobCover and has a different scale effect. At the same time, the *HT* of the two datasets were decreased, indicating that the landscape heterogeneity of Anhui Province was reduced. The diversity also reduced from 2005 to 2009, and MCD12Q1 was more sensitive to landscape heterogeneity and decreased more. While the *MPFD* of the two datasets are larger, and the values in 2005–2009 are slightly lower. Landscape patch type 'forestland', 'grassland', and 'cropland' area changes significantly during 2005 to 2009, indicating that human activities on the land reform frequently.

Table 9. Analysis of landscape indices based on MCD12Q1 and GlobCover data in Anhui Province of 2005–2009, at landscape-scale.

Landscape Index	MCD12Q1		GlobCover	
	2005	**2009**	**2005**	**2009**
F	0.0668	0.0600	0.0524	0.0563
HT	0.9642	0.9053	0.8867	0.8751
MPFD	1.0228	1.0203	1.0249	1.0221

3.3. Driving Force Analysis

The current integrity of the planet is being stressed beyond its biological capacity, and it is more essential now to understand the interaction between human activities and natural landscapes than ever [46]. DFA is considered to be an important tool for investigating the landscape pattern and changes [47]. The changes in the natural environment, human and social activities will impact on the structure of land cover. These changes can also cause the spatial changes of landscape pattern. In comparison with natural driving factors, human activities produce more effects on landscape pattern dynamics for land cover types, especially for a relatively short period of time [48–50].

Landscape change associated with exponential population growth poses major challenges to coupled human and natural systems [51]. 'Artificial area', 'wetland', and 'cropland' are the primary land covers that are apt to be affected by human activities. We just consider the affecting factors of the three types according to the 2005–2009 statistical yearbook data. The transportation length of railway, road, and inner river is just used to reflect the changes of 'artificial area'. It was 80,747 km in 2005, according to Anhui Statistical Yearbook, but increased to 157,316 km in 2009. It is obvious that human activities have greatly affected the landscape pattern. The study area is divided into five major landforms in the Huaihe River Plain, Jianghuai Hilly and Hilly Areas, Wanxi Mountain Hills, Wuliang Plain, and Wannan Hilly Mountains. The main nature reserves are mainly distributed in the plains along the Yangtze River and the hilly areas of southern Anhui. During the years 2005–2009, the number of nature reserves in the study area increased from 31 to 38, and the total area increased from 0.35 km^2 to 0.44 km^2. According to the landscape index analysis, the *NP* of the 'wetland' increased by 125 and 62, respectively, while the *PD* increased by 0.05 and 0.02. Also, *ED*, *LSI* and *PAFRAC* changed from 181.98, 40.6286, and 1.5147 in 2005 to 164.39, 36.3044, and 1.5116, in 2009, respectively. According to the 2005–2009 statistical yearbook data, population density increased from 466.76 people/km^2 to 486.75 people/km^2, and agricultural population also increased annually from 51.48 million in 2005 to 52.78 million in 2009. Over the four-year period, the cropland area increased from 40,924.51 to 41,712.22 km^2. The land use mode changed from extensive to intensive, corresponding to the *F* decreasing from 0.0668 in 2005 to 0.0600 in 2009. Conversely, the *CLUMPY* of 'cropland' increased from 0.8995 to 0.9095.

4. Conclusions

Both MCD12Q1 and GlobCover of 2005 and 2009 are comparatively used to identify the landscape pattern dynamics on land cover at a provincial scale. To form unified land cover types, it is highly necessary to harmonize the original LCCSs and generate the same resolution maps for the two datasets. It is hardly inevitable that some obvious differences can be found for some land cover types (e.g., forestland, cropland), due to various LCCSs, remotely sensed imagery and validation techniques. It will be more convincing to track the dynamics of landscape pattern by selecting certain types with the minimum difference among different GLC products. In general, we can find that there are slight differences for the reclassified land cover types between the two datasets over a relatively short time period. Nevertheless, there are still obvious differences for some land cover types. For example, there are significant differences for 'forestland' and 'cropland' in comparison with other types. They can be also used to reflect the dynamics of landscape pattern to a certain degree. By contrast, it will have more significance to compare the landscape pattern dynamics of land cover using a certain GLC product with longer time series (e.g., MCD12Q1). In addition, DFA is also an important tool to investigate the changes of landscape patterns. The impact of human activates on landscape pattern (e.g., cropland, artificial area, wetland) is more significant compared with the natural factors during a relatively short period of time.

Author Contributions: Jinling Zhao has gathered the experimental data and processed the time series global land cover products; Jie Wang wrote the introduction; Yu Jin unified the land cover classification schemes of GlobCover and MCD12Q1; Lingling Fan finished some of the results part for landscape-scale analysis; Chao Xu selected landscape indices; Dong Liang performed the driving force analysis of landscape pattern change; Linsheng Huang designed the general technical workflow and wrote the conclusion. All of the authors have read and approved the final manuscript.

Acknowledgments: This work was supported by Anhui Provincial Major Scientific and Technological Special Project (17030701062), Natural Science Research Project of Anhui Provincial Education Department (KJ2018A0009), and National Key Research and Development Program of China (2016YFD0800904).

Conflicts of Interest: The authors declare no conflict of interest.

References

1. Turner, M.G.; O'Neill, R.V.; Gardner, R.H.; Milne, B.T. Effects of changing spatial scale on the analysis of landscape pattern. *Landsc. Ecol.* **1989**, *3*, 153–162. [CrossRef]
2. Turner, M.G. Landscape ecology: The effect of pattern on process. *Annu. Rev. Ecol. Syst.* **1989**, *20*, 171–197. [CrossRef]
3. Pickett, S.T.; Cadenasso, M.L. Landscape ecology: Spatial heterogeneity in ecological systems. *Science* **1995**, *269*, 331. [CrossRef] [PubMed]
4. Teixidó, N.; Garrabou, J.; Arntz, W.E. Spatial pattern quantification of Antarctic benthic communities using landscape indices. *Mar. Ecol. Prog. Ser.* **2002**, *242*, 1–14. [CrossRef]
5. Hamstead, Z.A.; Kremer, P.; Larondelle, N.; McPhearson, T.; Haase, D. Classification of the heterogeneous structure of urban landscapes (STURLA) as an indicator of landscape function applied to surface temperature in New York City. *Ecol. Indic.* **2016**, *70*, 574–585. [CrossRef]
6. Opdam, P.; Steingröver, E.; Van Rooij, S. Ecological networks: A spatial concept for multi-actor planning of sustainable landscapes. *Landsc. Urban Plan.* **2006**, *75*, 322–332. [CrossRef]
7. Kerr, J.T.; Ostrovsky, M. From space to species: Ecological applications for remote sensing. *Trends Ecol. Evol.* **2003**, *18*, 299–305. [CrossRef]
8. Fagerholm, N.; Oteros-Rozas, E.; Raymond, C.M.; Torralba, M.; Moreno, G.; Plieninger, T. Assessing linkages between ecosystem services, land-use and well-being in an agroforestry landscape using public participation GIS. *Appl. Geogr.* **2016**, *74*, 30–46. [CrossRef]
9. Fernández, P.; Rodríguez, A.; Obregón, R.; de Haro, S.; Jordano, D.; Fernández-Haeger, J. Fine scale movements of the butterfly Plebejus argus in a heterogeneous natural landscape as revealed by GPS tracking. *J. Insect Behav.* **2016**, *29*, 80–98. [CrossRef]
10. Balthazar, V.; Vanacker, V.; Molina, A.; Lambin, E.F. Impacts of forest cover change on ecosystem services in high Andean mountains. *Ecol. Indic.* **2015**, *48*, 63–75. [CrossRef]
11. Vogelmann, J.E.; Helder, D.; Morfitt, R.; Choate, M.J.; Merchant, J.W.; Bulley, H. Effects of Landsat 5 Thematic Mapper and Landsat 7 Enhanced Thematic Mapper Plus radiometric and geometric calibrations and corrections on landscape characterization. *Remote Sens. Environ.* **2001**, *78*, 55–70. [CrossRef]
12. Fichera, C.R.; Modica, G.; Pollino, M. Land Cover classification and change-detection analysis using multi-temporal remote sensed imagery and landscape metrics. *Eur. J. Remote Sens.* **2012**, *45*, 1–18. [CrossRef]
13. Li, J.; Song, C.; Cao, L.; Zhu, F.; Meng, X.; Wu, J. Impacts of landscape structure on surface urban heat islands: A case study of Shanghai, China. *Remote Sens. Environ.* **2011**, *115*, 3249–3263. [CrossRef]
14. Qian, Y.; Zhou, W.; Yu, W.; Pickett, S.T. Quantifying spatiotemporal pattern of urban greenspace: New insights from high resolution data. *Landsc. Ecol.* **2015**, *30*, 1165–1173. [CrossRef]
15. Del Castillo, E.M.; García-Martin, A.; Aladrén, L.A.L.; de Luis, M. Evaluation of forest cover change using remote sensing techniques and landscape metrics in Moncayo Natural Park (Spain). *Appl. Geogr.* **2015**, *62*, 247–255. [CrossRef]
16. Herold, M.; Scepan, J.; Clarke, K.C. The use of remote sensing and landscape metrics to describe structures and changes in urban land uses. *Environ. Plan. A* **2002**, *34*, 1443–1458. [CrossRef]
17. Shao, G.; Wu, J. On the accuracy of landscape pattern analysis using remote sensing data. *Landsc. Ecol.* **2008**, *23*, 505–511.
18. Banerjee, R.; Srivastava, P.K. Reconstruction of contested landscape: Detecting land cover transformation hosting cultural heritage sites from Central India using remote sensing. *Land Use Policy* **2013**, *34*, 193–203. [CrossRef]
19. García-Llamas, P.; Calvo, L.; Álvarez-Martínez, J.M.; Suárez-Seoane, S. Using remote sensing products to classify landscape. A multi-spatial resolution approach. *Int. J. Appl. Earth Obs.* **2016**, *50*, 95–105. [CrossRef]
20. Reger, B.; Otte, A.; Waldhardt, R. Identifying patterns of land-cover change and their physical attributes in a marginal European landscape. *Landsc. Urban Plan.* **2007**, *81*, 104–113. [CrossRef]

21. Loveland, T.R.; Belward, A.S. The international geosphere biosphere programme data and information system global land cover data set (DISCover). *Acta Astronaut.* **1997**, *41*, 681–689. [CrossRef]
22. Hansen, M.C.; DeFries, R.S.; Townshend, J.R.G.; Sohlberg, R. Global land cover classification at 1 km spatial resolution using a classification tree approach. *Int. J. Remote Sens.* **2000**, *21*, 1331–1364. [CrossRef]
23. Friedl, M.A.; Sulla-Menashe, D.; Tan, B.; Schneider, A.; Ramankutty, N.; Sibley, A.; Huang, X. MODIS Collection 5 global land cover: Algorithm refinements and characterization of new datasets. *Remote Sens. Environ.* **2010**, *114*, 168–182. [CrossRef]
24. Bartholomé, E.; Belward, A.S. GLC2000: A new approach to global land cover mapping from Earth observation data. *Int. J. Remote Sens.* **2005**, *26*, 1959–1977. [CrossRef]
25. Defourny, P.; Vancutsem, C.; Bicheron, P.; Brockmann, C.; Nino, F.; Schouten, L.; Leroy, M. GLOBCOVER: A 300 m global land cover product for 2005 using Envisat MERIS time series. In Proceedings of the ISPRS Commission VII Mid-Term Symposium, Remote Sensing: From Pixels to Processes, Enschede, The Netherlands, 8–11 May 2006.
26. Chen, J.; Chen, J.; Liao, A.; Cao, X.; Chen, L.; Chen, X.; He, C.; Han, G.; Peng, S.; Lu, M.; Zhang, W.; Tong, X.; Mills, J. Global land cover mapping at 30 m resolution: A POK-based operational approach. *ISPRS J. Photogramm. Remote Sens.* **2015**, *103*, 7–27. [CrossRef]
27. Kupfer, J.A. Rethinking landscape metrics in a post-FRAGSTATS landscape. *Prog. Phys. Geogr.* **2012**, *36*, 400–420. [CrossRef]
28. Cushman, S.A.; McGarigal, K.; Neel, M.C. Parsimony in landscape metrics: Strength, universality, and consistency. *Ecol. Indic.* **2008**, *8*, 691–703. [CrossRef]
29. Ji, W.; Ma, J.; Twibell, R.W.; Underhill, K. Characterizing urban sprawl using multi-stage remote sensing images and landscape metrics. *Comput. Environ. Urban* **2006**, *30*, 861–879. [CrossRef]
30. Gillanders, S.N.; Coops, N.C.; Wulder, M.A.; Gergel, S.E.; Nelson, T. Multitemporal remote sensing of landscape dynamics and pattern change: Describing natural and anthropogenic trends. *Prog. Phys. Geog.* **2008**, *32*, 503–528. [CrossRef]
31. Zhang, S.; Fan, W.; Li, Y.; Yi, Y. The influence of changes in land use and landscape patterns on soil erosion in a watershed. *Sci. Total Environ.* **2017**, *574*, 34–45. [CrossRef] [PubMed]
32. Liang, D.; Zuo, Y.; Huang, L.S.; Zhao, J.L.; Teng, L.; Yang, F. Evaluation of the consistency of MODIS land cover product (MCD12Q1) based on Chinese 30 m GlobeLand30 datasets: A case study in Anhui Province, China. *ISPRS Int. J. Geo-Inf.* **2015**, *4*, 2519–2541. [CrossRef]
33. Ahmad, A.; Brown, G. Random projection random discretization ensembles—Ensembles of linear multivariate decision trees. *IEEE Trans. Knowl. Data Eng.* **2014**, *26*, 1225–1239. [CrossRef]
34. O'Neill, R.V.; Riitters, K.H.; Wickham, J.D.; Jones, K.B. Landscape pattern metrics and regional assessment. *Ecosyst. Health* **1999**, *5*, 225–233. [CrossRef]
35. Tischendorf, L.; Fahrig, L. How should we measure landscape connectivity? *Landsc. Ecol.* **2000**, *15*, 633–641. [CrossRef]
36. Jaeger, J.A. Landscape division, splitting index, and effective mesh size: New measures of landscape fragmentation. *Landsc. Ecol.* **2000**, *15*, 115–130. [CrossRef]
37. Rutledge, D. *Landscape Indices as Measures of the Effects of Fragmentation: Can Pattern Reflect Process?* Department of Conservation: Wellington, New Zealand, 2003; pp. 5–27.
38. McGarigal, K.; Cushman, S.A.; Ene, E. FRAGSTATS v4: Spatial Pattern Analysis Program for Categorical and Continuous Maps. Available online: http://www.umass.edu/landeco/research/fragstats/fragstats.html (accessed on 22 March 2018).
39. Wu, J. Effects of changing scale on landscape pattern analysis: Scaling relations. *Landsc. Ecol.* **2004**, *19*, 125–138. [CrossRef]
40. Patton, D.R. A diversity index for quantifying habitat "edge". *Wildl. Soc. Bull.* **1975**, *3*, 171–173.
41. Ramachandra, T.V.; Aithal, B.H.; Sanna, D.D. Insights to urban dynamics through landscape spatial pattern analysis. *Int. J. Appl. Earth Obs.* **2012**, *18*, 329–343.
42. Neel, M.C.; McGarigal, K.; Cushman, S.A. Behavior of class-level landscape metrics across gradients of class aggregation and area. *Landsc. Ecol.* **2004**, *19*, 435–455. [CrossRef]
43. Lausch, A.; Herzog, F. Applicability of landscape metrics for the monitoring of landscape change: Issues of scale, resolution and interpretability. *Ecol. Indic.* **2002**, *2*, 3–15.

44. Gustafson, E.J. Quantifying landscape spatial pattern: What is the state of the art. *Ecosystems* **1998**, *1*, 143–156. [CrossRef]
45. Crews-Meyer, K.A. Agricultural landscape change and stability in northeast Thailand: Historical patch-level analysis. *Agric. Ecosyst. Environ.* **2004**, *101*, 155–169. [CrossRef]
46. Shaker, R.R. The well-being of nations: An empirical assessment of sustainable urbanization for Europe. *Int. J. Sust. Dev. World* **2015**, *22*, 375–387. [CrossRef]
47. Eiter, S.; Potthoff, K. Landscape changes in Norwegian mountains: Increased and decreased accessibility, and their driving forces. *Land Use Policy* **2016**, *54*, 235–245. [CrossRef]
48. Gergel, S.E.; Turner, M.G.; Miller, J.R.; Melack, J.M.; Stanley, E.H. Landscape indicators of human impacts to riverine systems. *Aquat. Sci.* **2002**, *64*, 118–128. [CrossRef]
49. Alberti, M.; Marzluff, J.M.; Shulenberger, E.; Bradley, G.; Ryan, C.; Zumbrunnen, C. Integrating humans into ecology: Opportunities and challenges for studying urban ecosystems. *AIBS Bull.* **2003**, *53*, 1169–1179. [CrossRef]
50. Li, W.; Cao, Q.; Lang, K.; Wu, J. Linking potential heat source and sink to urban heat island: Heterogeneous effects of landscape pattern on land surface temperature. *Sci. Total Environ.* **2017**, *586*, 457–465. [CrossRef] [PubMed]
51. Shaker, R.R. Examining sustainable landscape function across the Republic of Moldova. *Habitat Int.* **2018**, *72*, 77–91. [CrossRef]